Journal of Nuclear Medicine, published on January 22, 2015 as doi:10.2967/jnumed.114.141648

PET imaging of translocator protein (18kDa) in a mouse model of Alzheimer's disease using ^{18}F-PBR06

Michelle L. James[†1,2], Nadia P. Belichenko[2], Thuy-Vi V. Nguyen[2], Lauren E. Andrews[1], Zhaoqing Ding[2,3], Hongguang Liu[1], Deepika Bodapati[1], Natasha Arksey[1], Bin Shen[1], Zhen Cheng[1], Tony Wyss-Coray[2,3], Sanjiv S. Gambhir[1], Frank M. Longo[2], Frederick T. Chin*[1].

[1]Molecular Imaging Program at Stanford (MIPS) Department of Radiology, Stanford University, Stanford, CA 94305-5484, USA

[2]Department of Neurology and Neurological Sciences, Stanford University, Stanford, CA 94305-5484, USA

[3]Veterans Administration Palo Alto Health Care System, CA 94304

*Corresponding author

Frederick T. Chin, 1201 Welch Road, Stanford, CA 94305-5484 (e-mail: chinf@stanford.edu).

[†]First Author: Michelle L. James, 3165 Porter Drive, Stanford, CA 94304. (e-mail: mljames@stanford.edu).

Running Foot Line: Imaging AD mice with 18F-PBR06

Figures/Tables: 7 Figures, 1 Table

Supplementary: 9 Figures

Word Count: 4979

Abstract

Herein we aim to evaluate the utility of ^{18}F-PBR06 for detecting alterations in translocator protein 18 kDa (TSPO), a biomarker of microglial activation, in a mouse model of Alzheimer's disease (AD). **Methods:** Wild-type (wt) and AD mice (i.e., APP$^{L/S}$) underwent ^{18}F-PBR06-PET imaging at predetermined time-points between the ages of 5-6 and 15-16 months. MR images were fused with PET/CT data to quantify ^{18}F-PBR06 uptake in hippocampus and cortex. *Ex vivo* autoradiography and TSPO/CD68 immunostaining was also performed using brain tissue from these mice. **Results:** PET images showed significantly higher accumulation of ^{18}F-PBR06 in cortex/hippocampus of 15-16 month old APP$^{L/S}$ mice compared to age-matched wts (cortex/muscle: 2.43 $\pm$ 0.19 vs 1.55 $\pm$ 0.15, $p<0.005$; hippocampus/muscle: 2.41 $\pm$ 0.13 vs 1.55 $\pm$ 0.12, $p<0.005$). And while no significant difference was found between wt and APP$^{L/S}$ mice aged ≤9-10 months using PET ($p=0.64$), we were able to visualize and quantify a significant difference in ^{18}F-PBR06 uptake in these mice using autoradiography (cortex/striatum: 1.13 $\pm$ 0.04 vs 0.96 $\pm$ 0.01, $p<0.05$; hippocampus/striatum: 1.266 $\pm$ 0.003 vs 1.096 $\pm$ 0.017, $p<0.001$). PET results for 15-16 month old mice correlated well with autoradiography and immunostaining – *i.e.,* increased ^{18}F-PBR06 uptake in brain regions containing elevated CD68 and TSPO staining in APP$^{L/S}$ mice compared to wts. **Conclusion:** ^{18}F-PBR06 shows great potential as a tool for visualizing TSPO/microglia in the progression and treatment of AD.

Keywords: microglial activation, Alzheimer's disease, translocator protein 18 kDa, PET.

INTRODUCTION

The main pathological hallmarks of Alzheimer's disease (AD) include senile plaques and neurofibrillary tangles, which are composed of toxic β-amyloid peptides and hyperphsophorylated tau aggregates respectively (*1*). Another key feature of AD is microglial activation – a complex cellular process responsible for the proinflammatory milieu known to promote neurotoxicity and neurodegeneration (*2*). Microglial activation is also involved in anti-inflammatory activity and can stimulate tissue repair (*3*). Much research is being conducted to better understand the role and various dynamic stages of microglial activation, however many questions remain.

Imaging techniques such as magnetic resonance imaging (MRI) and positron emission tomography (PET) provide a means to non-invasively visualize different structural/functional or molecular biomarkers, respectively, in living intact subjects (*4*). Such tools could enhance our understanding of the *in vivo* role of microglial activation in AD, and ultimately enable longitudinal monitoring of disease progression and response to therapies. Structural and functional MRI have provided numerous, valuable insights concerning brain atrophy, alterations in perfusion, and various brain networks in AD (*5*–*7*). However, due to the limited sensitivity of these techniques for detecting specific molecular alterations in a highly quantitative manner, MRI has not historically been the imaging modality of choice for visualizing microglia in AD.

PET imaging, on the other hand, using small molecule radioligands specific for the translocator protein 18 kDa (TSPO), has been used extensively to detect microglial activation in both preclinical and clinical studies (*8*). The TSPO is mainly located on the outer mitochondrial membrane and is involved in steroid biosynthesis under normal physiological conditions (*9*). While there are only moderate levels of TSPO in the healthy brain, these levels are increased under neuro-inflammatory/degenerative conditions (*10*,*11*). The predominant cell type expressing TSPO at regions of central nervous system pathology are activated microglia, therefore enabling TSPO-PET radioligands to serve as a useful index of microglial activation and neuroinflammation (*12*). PET imaging with the TSPO radioligand N-sec-Butyl-1-(2-chlorophenyl)-N-(11C)methyl-3-isoquinolinecarboxamide (^{11}C-PK11195) has been used as a non-invasive sensor of microglial activation in multiple conditions including AD (*13*). And although ^{11}C-PK11195 has provided useful information, its poor brain permeability and high plasma protein binding have limited its sensitivity and overall usefulness (*14*). Several improved TSPO tracers have been developed over the past decade (*15*), including N-(2,5-dimethoxybenzyl)-2-(18F)fluoro-N-(2-phenoxyphenyl)acetamide (^{18}F-PBR06) (*16*). ^{18}F-PBR06 has high affinity and specificity for TSPO across multiple species, and has been used in human studies for quantitation of brain TSPO (*17*). To date, no studies have been published

reporting the use of ^{18}F-PBR06 in AD patients or transgenic mouse models of AD.

The aim of this study is to evaluate the sensitivity and accuracy of ^{18}F-PBR06-PET for detecting alterations in TSPO levels in an accelerated mouse model of AD – i.e., Thy1-hAPP$^{Lond/Swe}$ (APP$^{L/S}$)(*18*) – at different stages of disease. We chose the cortex and hippocampus as areas of interest for these studies since they are the key brain structures containing AD pathology in this mouse model (*18*).

MATERIALS AND METHODS

General

If not otherwise stated, chemicals were purchased from commercial sources and used without further purification. PET imaging of mice was performed using microPET/CT (Inveon, Siemens). PET images were reconstructed by performing 2 iterations of 3-dimensional ordered subsets expectation maximization algorithm (12 subsets) and then 18 iterations of the accelerated version of 3D-maximum a posteriori – matrix size of 128 × 128 × 159. Attenuation correction was applied to dataset from CT image. PET images were co-registered with CT and MRI images using Inveon Research Workplace image analysis software version 4.0.

Study Design and Rationale

This study was designed to provide crucial information for planning future therapy monitoring studies with ^{18}F-PBR06 in APP$^{L/S}$ mice. Long-

term, we plan to evaluate numerous TSPO radiotracers side-by-side in therapy monitoring studies to determine which tracer can potentially serve as a clinical endpoint for novel AD therapeutics that alter microglial activation.

Toward this goal, we set out to evaluate whether ^{18}F-PBR06 can detect differences between APP$^{L/S}$ and wild-type (wt) mice aged 9-10 and 15-16 months, which will be the age of mice at the end of our planned therapy monitoring studies. These studies will involve a 3-4 month long treatment of wt/APP$^{L/S}$ mice aged 5-6 months (when mature amyloid plaques have formed in cortex and are starting to form in hippocampus (*18*)), and at 12-13 months (relatively late stage of disease exhibiting extensive AD pathology). These time points are based on previous published/unpublished work demonstrating efficacy of LM11A-31 (novel AD therapeutic that attenuates neuronal degeneration and microglial activation) in APP$^{L/S}$ mice at these ages (*19*). We designed the current study with two separate cohorts to maximize the amount of PET, autoradiography, and histological data we could acquire for our two primary ages of interest. See supplementary for information on the APP$^{L/S}$ mouse model of AD we chose for the current studies.

Small Animal Magnetic Resonance Imaging (MRI)

Brain MR images were acquired to provide an anatomical reference frame for each mouse so that we could draw accurate regions of interest

(ROIs) around the cortex and hippocampus during PET image analysis. Supplementary Figure 1 shows how all ROIs were drawn. Mice were scanned with a dedicated small animal 7 Tesla Varian Magnex Scientific MR scanner with custom-designed pulse sequences and radiofrequency coils using standard methods. See supplementary for details.

MicroPET/CT

^{18}F-PBR06 was synthesized via nucleophilic aliphatic substitution as previously described (*16*,*20*), with non decay-corrected radiochemical yield of 2.17 ± 0.38% and a specific radioactivity of 131.91 ± 16.09 GBq/μmol at end of bombardment (*n* = 8).

Mice were anesthetized using isoflurane gas (2.0-3.0% for induction and 1.5-2.5% for maintenance). Dynamic scans for 15-16 month old wt and APP$^{L/S}$ mice (*n* = 4 per group) were commenced just prior to intravenous administration of ^{18}F-PBR06 (5.5-7.5 MBq) and acquired in list mode format over 60 min. The resulting data was sorted into 0.5-mm sinogram bins and 19 time frames for image reconstruction (4 × 15 s, 4 × 60 s, 11 × 300 s). Blocking studies involved pre-treating 15-16 month old APP$^{L/S}$ mice (*n* = 3) with PK11195 (1 mg/kg, Sigma Aldrich) 10 min prior to radioligand administration. Static PET scans (10 min) were acquired 40 min after intravenous administration of ^{18}F-PBR06 (5.5-7.5 MBq). CT images were acquired just prior to each PET scan to provide an anatomical reference for PET data.

PET images were analyzed by drawing 3-dimensional regions around whole brain, muscle, cortex, and hippocampus (supplementary Fig. 1). The latter two regions were drawn between bregma +1.94 and +0.02 and bregma -1.22 and -2.30 respectively, to ensure consistency between mice. Percentage of injected dose per gram (%ID/g) was calculated for each region of interest. Signal-to-background ratios were calculated by dividing the uptake in each brain region by uptake in a reference region (i.e., muscle or whole brain). See supplementary figures 2-6 for how and why reference regions were selected.

Ex Vivo Autoradiography

Following final PET/CT scans, mice were perfused, brain tissue was embedded in optimal-cutting temperature compound (OCT, Tissue-Tek), and coronal sections (20 μm) were obtained for autoradiography. Autoradiography was conducted using previously described methods (*21*) and anatomy of brain sections was confirmed by Nissl staining.

For quantitation of autoradiography, we analyzed five sections per mouse aged 9-10 months (n = 3 per genotype) and five sections per mouse aged 15-16 months (n = 4 per genotype). For each section, one region was drawn within the somatosensory cortex, striatum, hippocampus, and choroid plexus (between bregma +1.94 and -2.30 – corresponding to brain regions used for PET image analysis), resulting in a mean signal intensity value for each brain region within each section. For each mouse, the mean signal intensities for cortex, hippocampus, and

choroid plexus were normalized to the mean signal intensity for striatum. The striatum contains low TSPO in this mouse model, and can therefore be used as an internal reference region to provide a signal-to-background ratio for each region of interest. See supplementary figure 7 for evidence of negligible TSPO staining in striatum of 15-16 month old wt and $APP^{L/S}$ mice.

Plasma Free Fraction (f_P)

Plasma free fraction (f_P) studies for ^{18}F-PBR06 in 15-16 month old mice (*n* = 3 $APP^{L/S}$, *n* = 4 wt) were performed at room temperature with ultrafiltration units, according to previously described methods (*22*).

CD68 and TSPO Staining

Frozen 50 μm coronal brain sections were collected using Microm HM 450 sliding microtome (Thermo Scientific). Free floating sections were incubated with either rat anti-CD68 (AbD Serotec; 1:1000) or rabbit anti-TSPO (Epitomics; 1:500). For visualization, sections were immersed in an avidin-biotin complex solution (Vector Laboratories) followed by 0.05% diaminobenzidine (Sigma) in TBS with 0.03% H_2O_2. See supplementary for CD68 and TSPO staining quantitation methods.

Statistics

All data are presented as mean ± SEM. Statistical analyses of data were performed using Wilcoxon-Mann-Whitney test within PRISM version

6.0d. Significance was set at $p<0.05$. *p = <0.05, **p = <0.005, and ***p = <0.0005, unless otherwise specified.

RESULTS

Small Animal PET

Dynamic ^{18}F-PBR06 imaging studies were performed with 15-16 month old APP$^{L/S}$ mice, known to exhibit extensive microglial activation. These studies were conducted to gain an understanding of the uptake, kinetics, and suitability of this tracer for detecting neuroinflammation in this mouse model of AD. Time activity curves generated from these studies (Fig. 1a) showed significantly higher ^{18}F-PBR06 accumulation in cortex and hippocampus of APP$^{L/S}$ mice compared to wts (cortex: 3.32 %ID/g $\pm$ 0.16 vs. 2.42 %ID/g $\pm$ 0.10, $p<0.005$; hippocampus: 3.65 %ID/g $\pm$ 0.17 vs. 2.54 %ID/g $\pm$ 0.12, $p<0.005$, at 40-50 min p.i., *n* = 4 per group). Pre-treating these same APP$^{L/S}$ mice with a known TSPO ligand, PK11195 (1 mg/kg), prior to tracer administration, dramatically reduced ^{18}F-PBR06-PET signal in cortex and hippocampus (52% reduction compared to baseline data summed between 40-50 min, $p<0.0001$) (Fig. 1b).

The sensitivity of ^{18}F-PBR06 for detecting TSPO in APP$^{L/S}$ mice was investigated by conducting PET studies in mice of different ages, exhibiting varying levels of microglial activation. Quantitation of PET images from these studies showed no significant difference in whole brain signal between APP$^{L/S}$ and wt mice 5-6 and 9-10 months old (supplementary Fig. 2). However, there was a significant difference

between $APP^{L/S}$ and wt mice aged ≥14-15 months (14-15 months: 1.51 %ID/g ± 0.08 vs. 1.28 %ID/g ± 0.05, $p<0.05$, n = 12 per group; 15-16 months: 1.41 %ID/g ± 0.06 vs. 1.06 %ID/g ± 0.10, $p<0.05$, n = 8 $APP^{L/S}$, n = 7 wt).

Next we quantified tracer accumulation in our pre-defined regions of interest (cortex and hippocampus) and found no significant difference in PET signal for 9-10 month old $APP^{L/S}$ and wt mice ($p = 0.64$) (Fig. 2). There was however, significantly higher ^{18}F-PBR06 accumulation in cortex and hippocampus of 15-16 month old $APP^{L/S}$ mice. This was demonstrated by %ID/g values (supplementary Fig. 3) and signal-to-background ratios using either muscle (Fig. 2) or whole brain as a reference region (supplementary Fig. 3). Cortex/muscle: 2.43 ± 0.19 vs 1.55 ± 0.15, $p<0.005$; hippocampus/muscle: 2.41 ± 0.13 vs 1.55 ± 0.12, $p<0.005$, n = 8 $APP^{L/S}$, n = 7 wt. Table 1 shows there was no significant difference in f_P for $APP^{L/S}$ versus wt mice aged 15-16 months ($p = 0.84$) (Table 1).

Ex Vivo Autoradiography

To further investigate the uptake of ^{18}F-PBR06 in specific brain regions at higher resolution we performed autoradiography immediately after PET imaging. Unlike PET results, quantitation of autoradiography images from 9-10 month old mice revealed significant elevation in ^{18}F-PBR06 uptake in cortex and hippocampus of $APP^{L/S}$ mice (Fig. 3)

(cortex/striatum: 1.13 ± 0.04 vs 0.96 ± 0.01, $p<0.05$; hippocampus/striatum: 1.266 ± 0.003 vs 1.096 ± 0.017, $p<0.001$, n = 3 per group). Whereas for 15-16 month old mice, autoradiography results (Fig. 4) were comparable to PET findings (Fig. 2), i.e., significantly higher ^{18}F-PBR06 accumulation in cortex and hippocampus of 15-16 month APP$^{L/S}$ compared to wts (cortex/striatum: 1.32 ± 0.04 vs 1.01 ± 0.02, $p<0.005$; hippocampus/striatum: 1.36 ± 0.06 vs 1.07 ± 0.01, $p<0.005$, n = 4 per group). Apart from the expected uptake in hippocampus/cortex, we also observed intense focal uptake in 1-3 small regions in almost all autoradiography images. Nissl staining of the same sections revealed that this focal uptake aligned with the choroid plexus. Visually, the uptake in choroid plexus appeared more intense in APP$^{L/S}$ mice compared to wts (from both age groups), and thus we decided to quantify this uptake. We found significantly higher ^{18}F-PBR06 choroid plexus uptake in APP$^{L/S}$ mice 15-16 months old compared to wt littermates (Fig. 4b,c)(1.99 ± 0.05 vs 1.53 ± 0.02 %ID/g, $p<0.005$, n = 4 per group), and a trend toward increased uptake in choroid plexus of 9-10 month old mice (Fig. 3b,c). Autoradiography results from PK11195 blocking study (Fig. 4a,b) show a marked reduction of ^{18}F-PBR06 uptake in all regions of 15-16 month old APP$^{L/S}$ mouse brain.

Immunohistochemistry

In order to assess whether ^{18}F-PBR06-PET signal correlated with levels of activated microglia and TSPO, we harvested brain tissue from 9-10 and 15-16 month old mice and performed immunohistochemistry (Fig. 5 and 6.). Quantitation of percent cortical/hippocampal area occupied by CD68 staining showed increased levels of activated microglia in APP$^{L/S}$ compared to wts for both 9-10 month old ($p<0.0005$, $n = 8$ per group) and 15-16 month old mice ($p<0.0005$, $n = 8$ per group). Likewise, the percent cortical/hippocampal area occupied by TSPO staining was found to be significantly greater in APP$^{L/S}$ mice compared to wts for 9-10 ($p<0.0005$, $n = 8$ per group) and 15-16 month old mice ($p<0.0005$, $n = 8$ per group).

Figure 7 and supplementary figure 8 show that autoradiography and PET results, for 15-16 month old mice, correlated well with each other (r^2=0.76) and also with immunostaining – *i.e.,* increased ^{18}F-PBR06 uptake in brain regions containing elevated CD68 and TSPO staining in APP$^{L/S}$ compared to wts. Specifically, we observed a strong/moderate correlation between PET signal and TSPO levels in cortex (r^2=0.90) and hippocampus (r^2=0.73), and also between PET signal and CD68 levels in cortex (r^2=0.91) and hippocampus (r^2=0.78). Additionally, we found a strong correlation between CD68 and TSPO staining in both cortex (r^2 = 0.87) and hippocampus (r^2 = 0.94) (supplementary Fig. 9).

DISCUSSION

Herein we assessed the sensitivity and accuracy of ^{18}F-PBR06-PET for detecting alterations in TSPO levels and microglial activation in a

well characterized, accelerated transgenic mouse model of AD (*18*). Our ultimate goal was to determine the potential of this tracer as a tool for investigating the *in vivo* role of microglia in AD, and as a surrogate marker for treatment response in future therapy-monitoring studies.

We found that ^{18}F-PBR06-PET could detect elevated TSPO and activated microglia in cortex and hippocampus of 15-16 month old APP$^{L/S}$ mice, as verified by *ex vivo* autoradiography and the strong correlation with TSPO/CD68 immunohistochemistry. The specificity of ^{18}F-PBR06 for TSPO in APP$^{L/S}$ mouse brain was confirmed by blocking studies with known TSPO ligand PK11195. Additionally we verified that the increased ^{18}F-PBR06 uptake in 15-16 month old APP$^{L/S}$ mice was not due to differences in f_P of the tracer between wt and diseased mice (Table 1.). Although we showed elevated CD68/TSPO staining in 9-10 month old APP$^{L/S}$ mice compared to wts, we did not detect elevated brain-PET signal in these mice. This was likely due to the limited spatial resolution of microPET and issues associated with the partial volume effect when quantifying radiotracer uptake in small regions (e.g., mouse brain structures) (*23*). It was not until we used *ex vivo* autoradiography, a technique with higher spatial resolution compared to PET, that we could visualize and quantify a significant difference in ^{18}F-PBR06 cortical/hippocampal uptake in these younger APP$^{L/S}$ mice compared to age-matched wts. Due to this finding, we plan to perform *ex vivo* autoradiography for all future mouse studies with ^{18}F-PBR06 to

complement our PET data. Mouse PET and autoradiography data will serve as a proof of principle so we can move into human AD patients as a next step (where resolution will be a lesser issue). Imaging rat models of AD could reduce partial volume related issues, however since these models have not been as useful for AD therapeutic development they are not suitable for our future planned therapy monitoring studies.

An unexpected finding from our autoradiography studies was that we could clearly visualize accumulation of ^{18}F-PBR06 in the choroid plexus, and that this uptake was significantly higher in 15-16 month old APP$^{L/S}$ mice compared to age-matched littermates. The choroid plexus contains moderate levels of TSPO in healthy human, monkey, and rodent brain (*24*), however not much is known about TSPO levels in this structure in disease. Since the choroid plexus is involved in filtering and producing cerebrospinal fluid, and its dysfunction has been linked to amyloid build-up in AD (*25*), our observation could be an indication of a molecular dysfunction/alteration in the choroid plexus of this mouse model of AD. Although there have been reports detailing the anatomical and functional changes of the choroid plexus in clinical AD cases (*26*), there have been no such reports detailing TSPO alterations in this structure in AD. Recently however, there was a study showing increased choroid plexus uptake of another TSPO PET radioligand, N-(2-Methoxybenzyl)-N-(6-phenoxy-3-pyridinyl)acetamide (^{11}C-PBR28), in temporal lobe epilepsy patients compared to healthy controls (*27*). Changes in TSPO expression

in choroid plexus could therefore play a role in (and/or serve as a molecular sensor for) different neurological diseases, and thus warrants further investigation.

There have been several PET imaging studies using TSPO radioligands in different mouse models of AD, which have provided useful information about the feasibility of imaging this target in AD mice, and also about which histological markers correlate with TSPO imaging. For example, Venneti and colleagues showed that ^{11}C-PK11195 brain uptake increased with age of their AD mice, and that the PET signal moderately correlated with levels of microglia as determined by Iba1 staining (r^2 = 0.59, p = 0.04) (*28*). More recently, Maeda demonstrated a strong relationship between N-benzyl-N-ethyl-2-(7-[11C]methyl-8-oxo-2-phenyl-7,8-dihydro-9H-purin-9- yl)acetamide (^{11}C-AC-5216) autoradiography and tau-induced neurodegeneration in PS19 AD mice (overexpressing mutant human tau) (*29*). In the latter study no significant differences were observed between TSPO-PET images of 24-month old wt and transgenic mice in cortex or hippocampus until normalized to the striatum. Whereas in our current studies with ^{18}F-PBR06, we observed a significant increase in cortical/hippocampal uptake in 15-16 month old transgenic mice compared to wts prior to normalization. Additionally, our current studies are the first to show a correlation between TSPO staining, activated microglia (via CD68 staining), and TSPO-PET signal in AD mice (Fig. 7).

This type of information is critical to understanding the *in vivo* accuracy of a PET tracer for its desired target.

Since the studies reported by Venneti and Maeda were conducted in different AD mouse models, it is difficult to draw conclusions about which TSPO tracer is most suitable for imaging neuroinflammation in AD. In order to better understand how different TSPO tracers compare to each other, we need to conduct systematic studies to evaluate the sensitivity and accuracy of TSPO tracers in the same AD mouse model.

We are currently planning to compare ^{18}F-PBR06 with newer TSPO radiotracers, such as *N*,*N*-diethyl-9-(2-(fluoro-^{18}*F*)ethyl)-5-methoxy-2,3,4,9-tetrahydro-1*H*-carbazole-4-carboxamide (^{18}F-GE180) (*30*), and other fluorine-18 TSPO tracers in the same APP$^{L/S}$ mice. Subsequent work will involve using the most sensitive TSPO-PET tracer for therapy monitoring studies to evaluate novel therapeutics that directly or indirectly affect neuroinflammation in both mouse and man.

Conclusion

This study is the first characterization of ^{18}F-PBR06 in a mouse model of AD. Results from this work provide definitive evidence that the observed PET signal in cortex and hippocampus of 15-16 month old APP$^{L/S}$ mice correlates, in both a temporal and spatial manner, with levels of TSPO and activated microglia. Although we could not visualize significant differences in ^{18}F-PBR06-PET signal in younger APP$^{L/S}$ mice (where levels of microglial activation were less pronounced), we were able

to quantify this difference using *ex vivo* autoradiography. These findings will certainly impact and guide future research involving the use of ^{18}F-PBR06 for imaging mouse models of AD, especially when selecting the age of mice for therapy monitoring studies and to ensure that high resolution *ex vivo* autoradiography is performed to complement microPET imaging data. Overall these results serve as a proof-of-principle, highlighting the potential of ^{18}F-PBR06-PET for imaging activated microglia/TSPO in the progression and treatment of AD. Studies investigating the use of this tracer in human AD patients and for screening/evaluating novel AD therapies in mice are currently underway.

Acknowledgements: We would like to thank Dr. Victor W. Pike and the National Institute of Mental Health (NIMH) for generously supplying precursor/standard for radiosynthesis of ^{18}F-PBR06. We also thank Dr. Timothy Doyle, Dr. Laura Pisani, and Dr. Frezghi Habte, from the small animal imaging facility (SAIF) at Stanford for their technical support with PET/CT, MRI, and image analysis, respectively.

Financial Support: Stanford University Department of Radiology internal funds (FTC), National Cancer Institute ICMIC P50 grant CA114747 (SSG), the Koret/Taube Foundations (FML), Jean Perkins Foundation (FML), and the Horngren Family (FML).

REFERENCES

1. Serrano-Pozo A, Frosch MP, Masliah E, Hyman BT. Neuropathological alterations in Alzheimer disease. *Cold Spring Harb Perspect Med*. 2011; 1:a006189.
2. Cameron B, Landreth GE. Inflammation, microglia, and Alzheimer's disease. *Neurobiol Dis*. 2010; 37:503–509.
3. Weitz TM, Town T. Microglia in Alzheimer's disease: it's all about context. *Int J Alzheimers Dis*. 2012; 2012:314185.
4. James ML, Gambhir SS. A molecular imaging primer: modalities, imaging agents, and applications. *Physiol Rev*. 2012; 92:897–965.
5. Filippi M, Agosta F, Frisoni GB, et al. Magnetic resonance imaging in Alzheimer's disease: from diagnosis to monitoring treatment effect. *Curr Alzheimer Res*. 2012; 9:1198–209.
6. Frisoni GB, Fox NC, Jack CR, Scheltens P, Thompson PM. The clinical use of structural MRI in Alzheimer disease. *Nat Rev Neurol*. 2010; 6:67–77.
7. Chen W, Song X, Beyea S, D'Arcy R, Zhang Y, Rockwood K. Advances in perfusion magnetic resonance imaging in Alzheimer's disease. *Alzheimer's Dement*. 2011; 7:185–196.
8. Chen MK, Guilarte TR. Translocator protein 18 kDa (TSPO): molecular sensor of brain injury and repair. *Pharmacol Ther*. 2008; 118:1–17.

9. Scarf AM, Kassiou M. The translocator protein. *J Nucl Med*. 2011; 52:677–680.

10. Benavides J, Fage D, Carter C, Scatton B. Peripheral type benzodiazepine binding sites are a sensitive indirect index of neuronal damage. *Brain Res*. 1987; 421:167–172.

11. Wilms H, Claasen J, Röhl C, Sievers J, Deuschl G, Lucius R. Involvement of benzodiazepine receptors in neuroinflammatory and neurodegenerative diseases: Evidence from activated microglial cells in vitro. *Neurobiol Dis*. 2003; 14:417–424.

12. Owen DRJ, Matthews PM. Imaging brain microglial activation using positron emission tomography and translocator protein-specific radioligands. *Int Rev Neurobiol*. 2011; 101:19–39.

13. Cagnin A, Brooks DJ, Kennedy AM, et al. In-vivo measurement of activated microglia in dementia. *Lancet*. 2001; 358:461–467.

14. Chauveau F, Boutin H, Van Camp N, Dollé F, Tavitian B. Nuclear imaging of neuroinflammation: a comprehensive review of [11C]PK11195 challengers. *Eur J Nucl Med Mol Imaging*. 2008; 35:2304–2319.

15. Luus C, Hanani R, Reynolds A, Kassiou M. The development of PET radioligands for imaging the translocator protein (18 kDa): What have we learned? *J Label Compd Radiopharm*. 2010; 53:501–510.

16. Briard E, Shah J, Musachio J. Synthesis and evaluation of a new 18F-labeled ligand for PET imaging of brain peripheral benzodiazepine receptors. *J Labeled Compd Radiopharm*. 2005; 48 (abstract).

17. Fujimura Y, Kimura Y, Siméon FG, et al. Biodistribution and radiation dosimetry in humans of a new PET ligand, 18F-PBR06, to image translocator protein (18 kDa). *J Nucl Med*. 2010; 51:145–149.

18. Rockenstein E, Mallory M, Mante M, Sisk A, Masliaha E. Early formation of mature amyloid-beta protein deposits in a mutant APP transgenic model depends on levels of abeta(1-42). *J Neurosci Res*. 2001; 66:573–582.

19. Nguyen T-V V, Shen L, Vander Griend L, et al. Small molecule p75NTR ligands reduce pathological phosphorylation and misfolding of tau, inflammatory changes, cholinergic degeneration, and cognitive deficits in ABPPL/S transgenic mice. *J Alzheimers Dis*. 2014; 42:459-483.

20. Lartey FM, Ahn GO, Shen B, et al. PET imaging of stroke-induced neuroinflammation in mice using [18F]PBR06. *Mol Imaging Biol*. 2014; 16:109–117.

21. James ML, Shen B, Zavaleta CL, et al. New positron emission tomography (PET) radioligand for imaging σ-1 receptors in living subjects. *J Med Chem*. 2012; 55:8272–8282.

22. Gandelman MS, Baldwin RM, Zoghbi SS, Zea-Ponce Y, Innis RB. Evaluation of ultrafiltration for the free-fraction determination of single photon emission computed tomography (SPECT) radiotracers: beta-CIT, IBF, and iomazenil. *J Pharm Sci*. 1994; 83:1014–1019.

23. Waerzeggers Y, Monfared P, Viel T, Winkeler A, Jacobs AH. Mouse models in neurological disorders: applications of non-invasive imaging. *Biochim Biophys Acta*. 2010; 1802:819–839.

24. Cymerman U, Pazos A, Palacios JM. Evidence for species differences in “peripheral” benzodiazepine receptors: an autoradiographic study. *Neurosci Lett*. 1986; 66:153–158.

25. Krzyzanowska A, Carro E. Pathological alteration in the choroid plexus of Alzheimer’s disease: implication for new therapy approaches. *Front Pharmacol*. 2012; 3:1–5.

26. Serot JM, Béné MC, Foliguet B, Faure GC. Morphological alterations of the choroid plexus in late-onset Alzheimer’s disease. *Acta Neuropathol*. 2000; 99:105–108.

27. Hirvonen J, Kreisl WC, Fujita M, et al. Increased in vivo expression of an inflammatory marker in temporal lobe epilepsy. *J Nucl Med*. 2012; 53:234–240.

28. Venneti S, Lopresti BJ, Wang G, et al. PK11195 labels activated microglia in Alzheimer’s disease and in vivo in a mouse model using PET. *Neurobiol Aging*. 2009; 30:1217–1226.

29. Maeda J, Zhang M-R, Okauchi T, et al. In vivo positron emission tomographic imaging of glial responses to amyloid-beta and tau pathologies in mouse models of Alzheimer's disease and related disorders. *J Neurosci*. 2011; 31:4720–4730.

30. Wadsworth H, Jones P a, Chau W-F, et al. [^{18}F]GE-180: a novel fluorine-18 labelled PET tracer for imaging translocator protein 18 kDa (TSPO). *Bioorg Med Chem Lett*. 2012; 22:1308–1313.

FIGURES

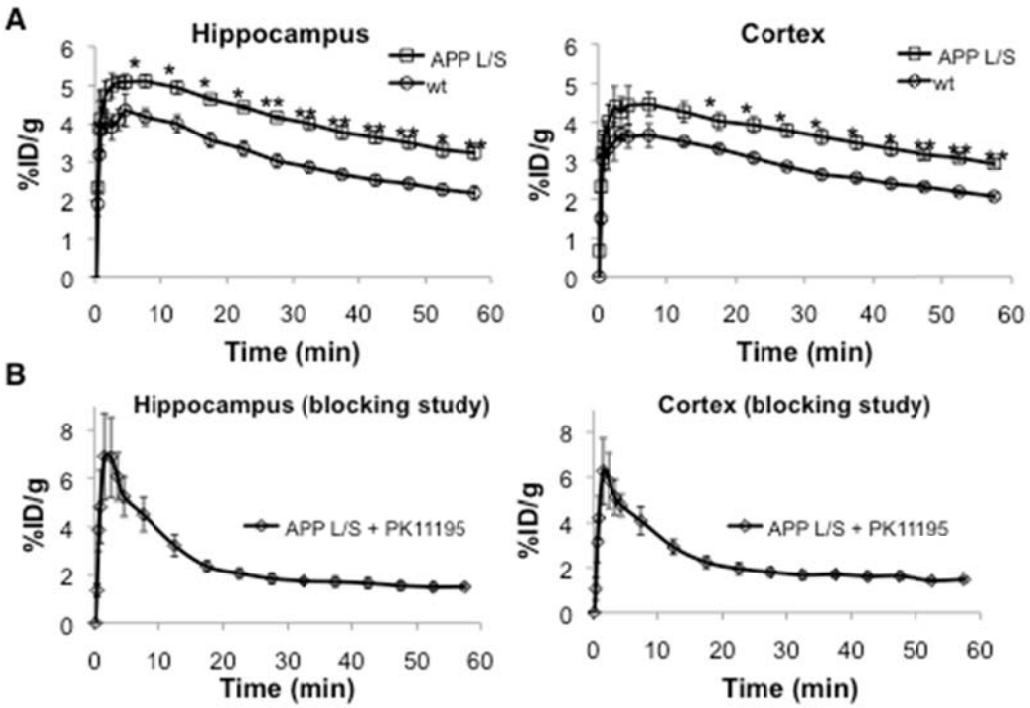

Figure 1. Time activity curves showing ^{18}F-PBR06 accumulation in (A) 15-16 month old APP$^{L/S}$ and wt mice, and (B) APP$^{L/S}$ mice following pre-treatment with PK11195. *p-value <0.05 **p-value <0.005.

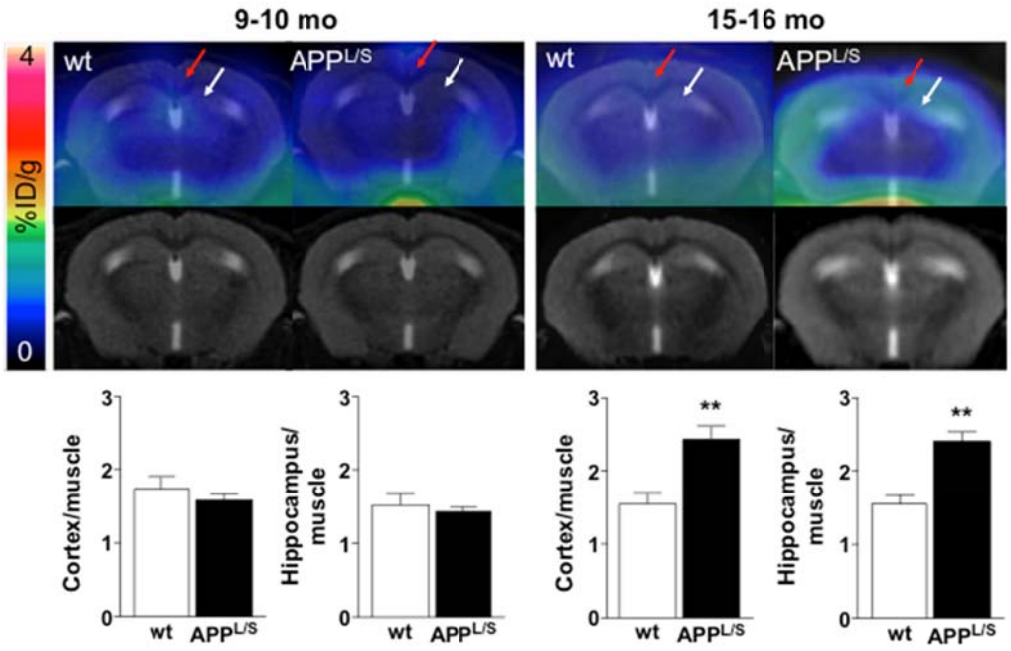

Figure 2. PET/MR images and graphs depicting ^{18}F-PBR06 accumulation in APP$^{L/S}$ versus wt mice 9-10 months (*n* = 7 per group) and 15-16 months of age (*n* = 8 APP$^{L/S}$, *n* = 7 wt). Red and white arrows point to cortex and hippocampus respectively. **p-value <0.005.

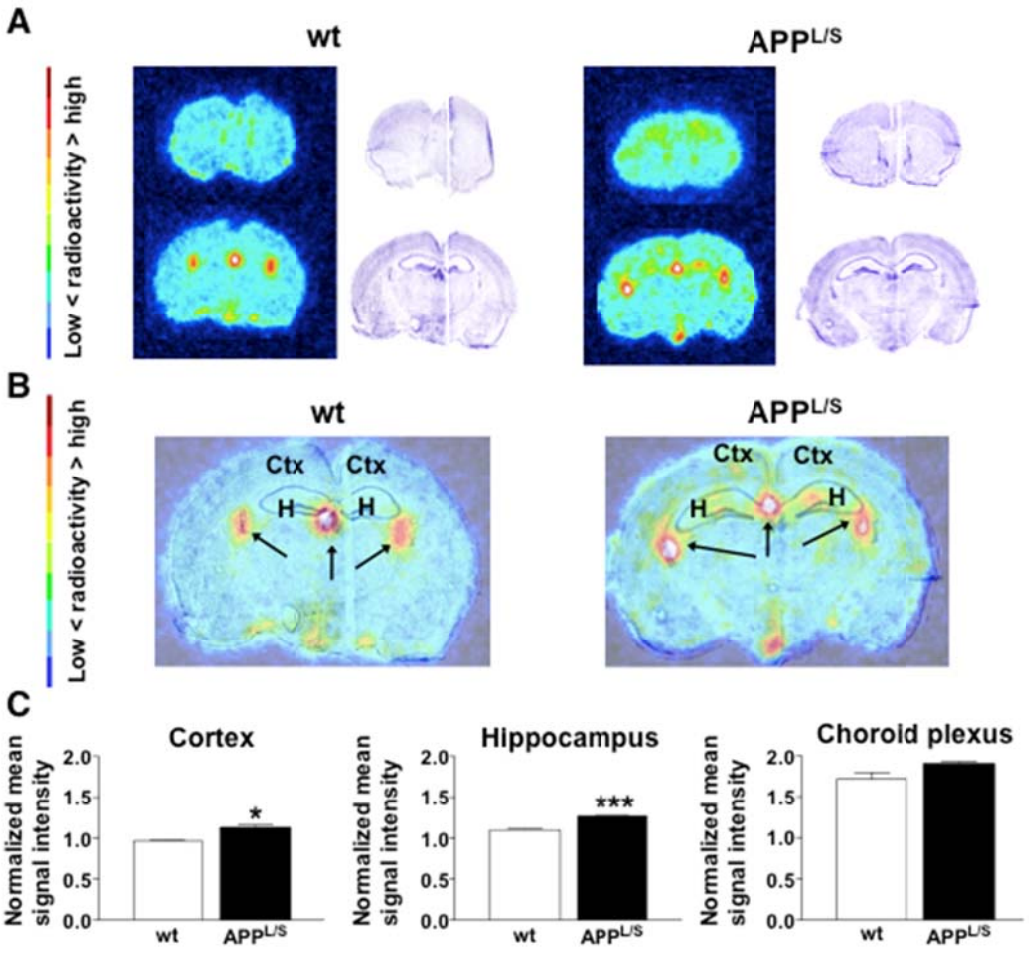

Figure 3. *Ex vivo* autoradiography of 9-10 month old mice. (A) Representative images and Nissl staining of same brain sections. (B) Overlay of autoradiography brain images with Nissl staining. (C) Mean signal intensity for specific brain regions normalized to striatum for wt and $APP^{L/S}$ mice (*n* = 3 per group). Ctx = cortex, H = hippocampus, arrows = choroid plexus. *p-value <0.05 ***p-value <0.0005.

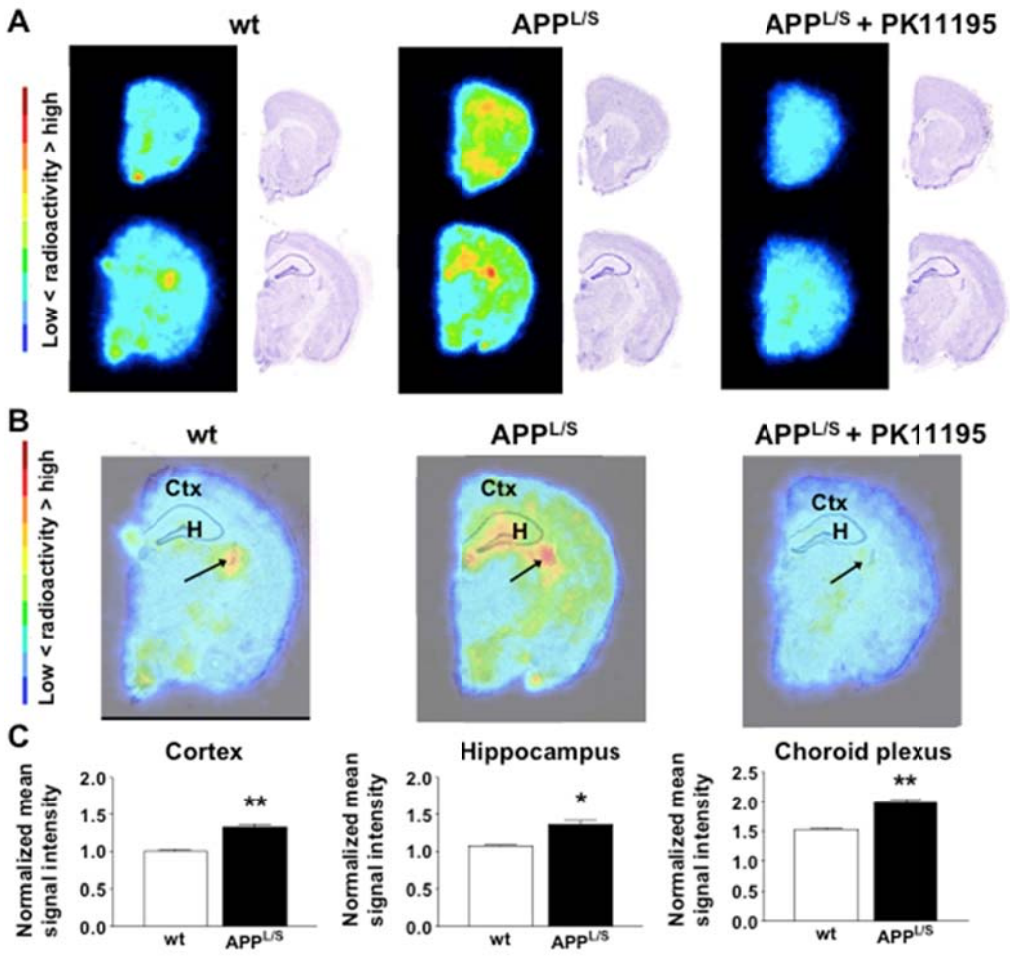

Figure 4. *Ex vivo* autoradiography of 15-16 month old mice. (A) Representative images and Nissl staining of same brain sections. (B) Overlay of autoradiography brain images with Nissl staining. (C) Mean signal intensity for specific brain regions normalized to striatum for wt and APP$^{L/S}$ mice (*n* = 4 per group). Ctx = cortex, H = hippocampus, arrows = choroid plexus. *p-value <0.05 **p-value <0.005.

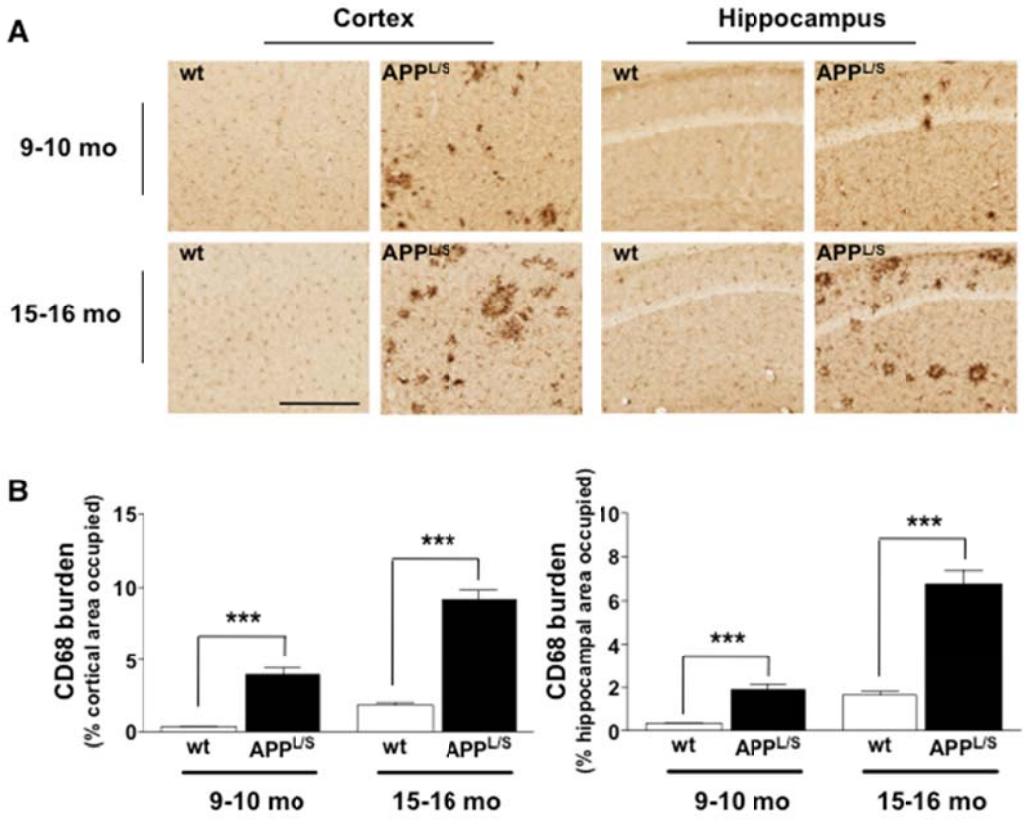

Figure 5. CD68 staining. (A) Representative 20x images from 9-10 and 15-16 month old $APP^{L/S}$ and wt mice (*n* = 8 per genotype). Scale bar = 250 μm. (B) Quantitation of percent cortical/hippocampal area occupied by CD68 staining. ***p-value <0.0005.

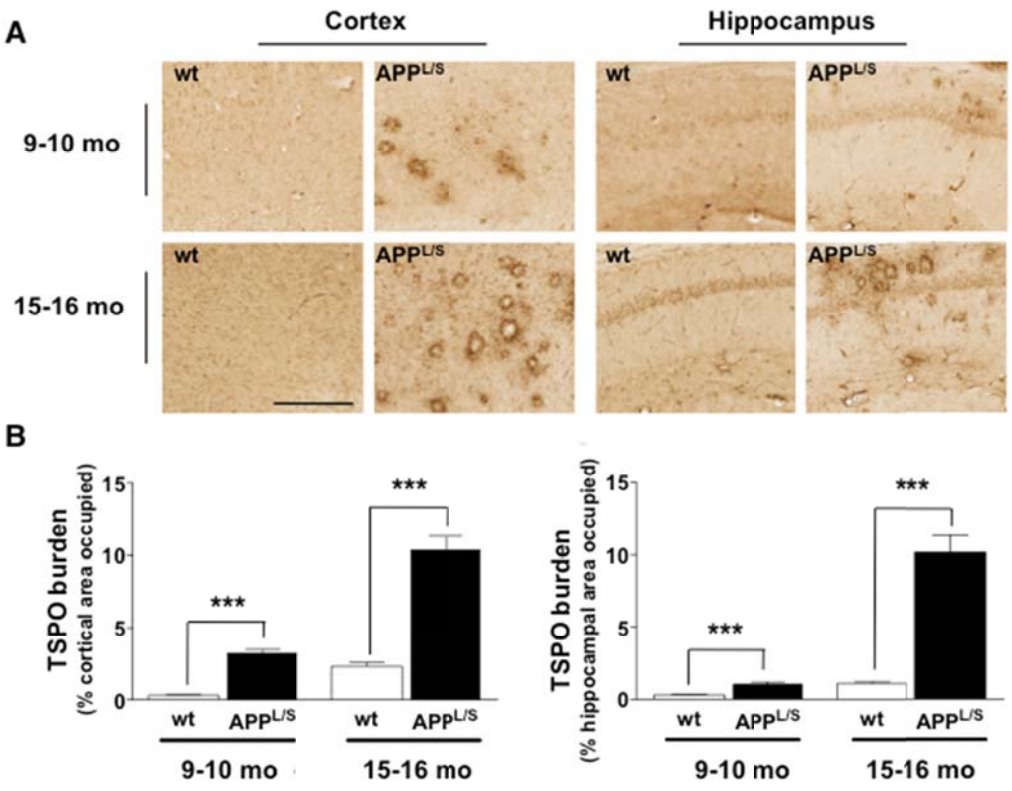

Figure 6. TSPO staining. (A) Representative 20x images from 9-10 and 15-16 month old mice $APP^{L/S}$ and wt mice (*n* = 8 per genotype). Scale bar = 250 μm. (B) Quantitation of percent cortical/hippocampal area occupied by TSPO staining. ***p-value <0.0005.

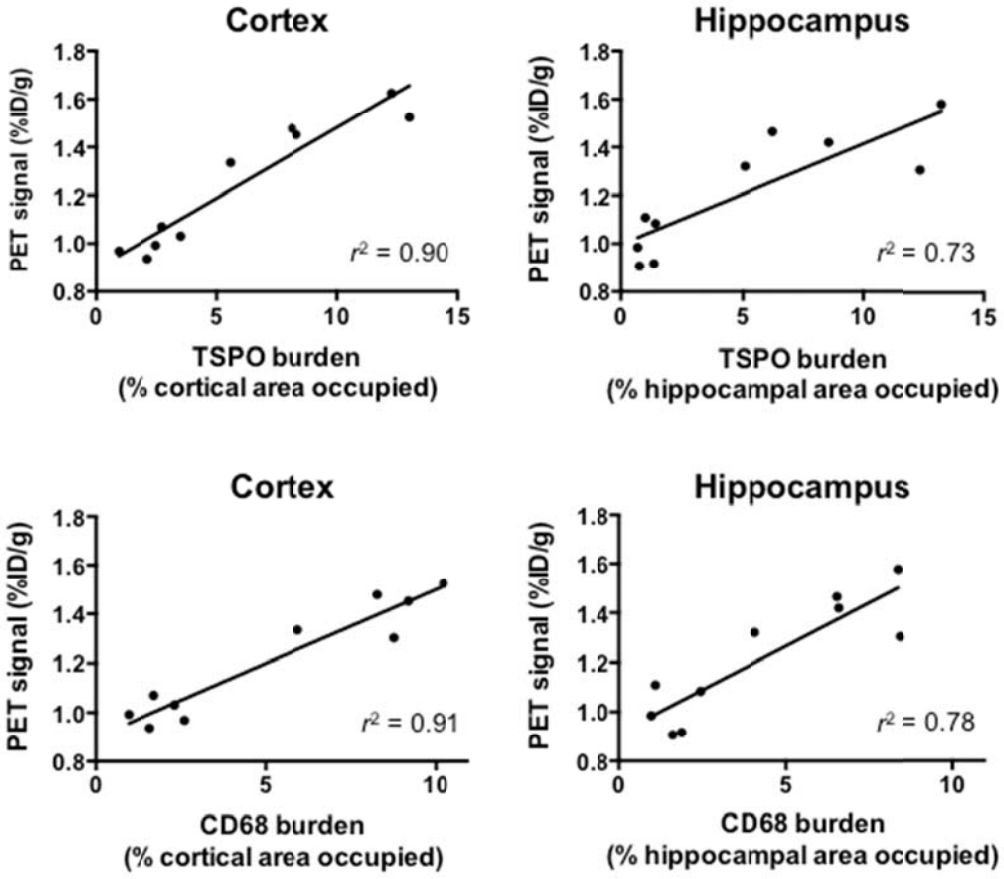

Figure 7. Correlation between TSPO/CD68 burden and PET signal for 15-16 month old $APP^{L/S}$ and wt mice (*n* = 5 per group).

Table 1. Plasma free fraction (f_P) of ^{18}F-PBR06 in 15-16 month old mice.

Genotype	f_P
wt	18.5 $\pm$ 0.5 (*n* = 4)
$APP^{L/S}$	18.7 $\pm$ 0.6 (*n* = 3)

Errors are represented as SEM.